© 2022. Published by The Company of Biologists Ltd | Development (2022) 149, dev200616. doi:10.1242/dev.200616

TECHNIQUES AND RESOURCES

RESEARCH ARTICLE

Breasi-CRISPR: an efficient genome-editing method to interrogate protein localization and protein–protein interactions in the embryonic mouse cortex

Brandon L. Meyerink[1,2], Pratiksha KC[1,*], Neeraj K. Tiwari[1,*], Claire M. Kittock[1,3], Abigail Klein[1,2], Claire M. Evans[4] and Louis-Jan Pilaz[1,3,‡]

ABSTRACT

In developing tissues, knowing the localization and interactors of proteins of interest is key to understanding their function. Here, we describe the Breasi-CRISPR approach (Brain Easi-CRISPR), combining Easi-CRISPR with *in utero* electroporation to tag endogenous proteins within embryonic mouse brains. Breasi-CRISPR enables knock-in of both short and long epitope tag sequences with high efficiency. We visualized epitope-tagged proteins with varied expression levels, such as ACTB, LMNB1, EMD, FMRP, NOTCH1 and RPL22. Detection was possible by immunohistochemistry as soon as 1 day after electroporation and we observed efficient gene editing in up to 50% of electroporated cells. Moreover, tagged proteins could be detected by immunoblotting in lysates from individual cortices. Next, we demonstrated that Breasi-CRISPR enables the tagging of proteins with fluorophores, allowing visualization of endogenous proteins by live imaging in organotypic brain slices. Finally, we used Breasi-CRISPR to perform co-immunoprecipitation mass-spectrometry analyses of the autism-related protein FMRP to discover its interactome in the embryonic cortex. Together, these data demonstrate that Breasi-CRISPR is a powerful tool with diverse applications that will propel the understanding of protein function in neurodevelopment.

KEY WORDS: CRISPR, Brain development, Radial glia, Neurons, *In utero* electroporation, FMRP

INTRODUCTION

Brain development involves a myriad of mechanisms and pathways, which rely heavily on proteins operating in defined subcellular compartments, via interactions with other molecules. The study of these mechanisms classically involves analyses such as immunohistochemistry (IHC) to characterize protein localization, and immunoprecipitation approaches to probe for protein interactors. However, studying endogenous proteins in the developing cortex remains challenging. This is especially the case when a protein of interest lacks specific antibodies to perform the aforementioned analyses. Overexpression of tagged proteins in subsets of cells has been used to circumvent this issue; however, protein overexpression can have drastic consequences on the cells of interest, preventing the experimenter from studying a protein in a physiological setting (Kintaka et al., 2016; Kafri et al., 2016). Moreover, having too much of a particular protein can lead to nonspecific binding to proteins with which it normally does not interact.

CRISPR technology has given researchers the opportunity to manipulate endogenous proteins to interrogate their function. In the developing mouse cortex, *in utero* electroporation (IUE) can be used to deliver the reagents necessary for CRISPR-based epitope tagging (Tsunekawa et al., 2016; Suzuki et al., 2016; Mikuni et al., 2016; Uemura et al., 2016; Fang et al., 2021). Some approaches rely on the homology-directed repair (HDR) machinery operating in early progenitor cells [embryonic day (E) 12-13] (Mikuni et al., 2016; Tsunekawa et al., 2016; Uemura et al., 2016), whereas others leverage the non-homologous end joining (NHEJ) machinery in late progenitor cells and post-mitotic neurons (E15 and beyond; Suzuki et al., 2016; Fang et al., 2021). For all these paradigms, CRISPR reagents consist of bi-cistronic expression vectors encoding a single guide RNA (sgRNA) and CRISPR-CAS9 protein, together with a separate DNA fragment to direct HDR or NHEJ to introduce a sequence of interest. Here, we couple IUE in the developing mouse cortex with the Easi-CRISPR approach (‘efficient additions with ssDNA inserts-CRISPR’; Miura et al., 2018; Quadros et al., 2017). Easi-CRISPR has mainly been used to generate transgenic mice by electroporating single-cell embryos with pre-formed RNP complexes composed of recombinant CAS9 and synthetic guide RNAs together with a chemically enhanced single-stranded oligo donor (Fig. 1A). We have applied this approach to the developing brain, electroporating neuronal precursors with these RNP complexes to edit neural clonal lineages selectively. We call this approach Breasi-CRISPR (‘Brain Easi-CRISPR’). We report that Breasi-CRISPR is an efficient and rapid method to introduce epitope-tagged sequences in cells of the developing cortex, enabling the visualization of endogenous protein in individual cells as soon as 1 day after electroporation in up to 50% of the electroporated cells, and in 30% of all the cells of the electroporated region. However, the more significant technical advance provided by this approach is that the high efficiency of recombination enables the detection of tagged proteins by immunoblot analyses in single cortices in as little as 2 days after electroporation and by IHC in as little as 24 h. To demonstrate further the power of this approach, we tagged endogenous proteins with EGFP to visualize them by live imaging in brains slices 2 days after IUE. Finally, we performed co-immunoprecipitation (co-IP) mass-spectrometry experiments with an endogenously epitope-tagged protein. These experiments led to

[1]Pediatrics and Rare Diseases Group, Sanford Research, Sioux Falls, SD 57104, USA. [2]Basic Biomedical Sciences, University of South Dakota Sanford School of Medicine, Vermillion, SD 57069, USA. [3]Sanford School of Medicine, University of South Dakota, Sioux Falls, SD 57105, USA. [4]Histology Core, Sanford Research, Sioux Falls, SD 57104, USA.
*These authors contributed equally to this work

‡Author for correspondence (ljpilaz@sanfordhealth.org)

B.L.M., 0000-0002-4058-1685; N.K.T., 0000-0002-3496-5148; C.M.K., 0000-0002-0554-0554; L.-J.P., 0000-0002-9035-1327

Handling Editor: François Guillemot
Received 2 February 2022; Accepted 15 August 2022

Development (2022) 149, dev200616. doi:10.1242/dev.200616

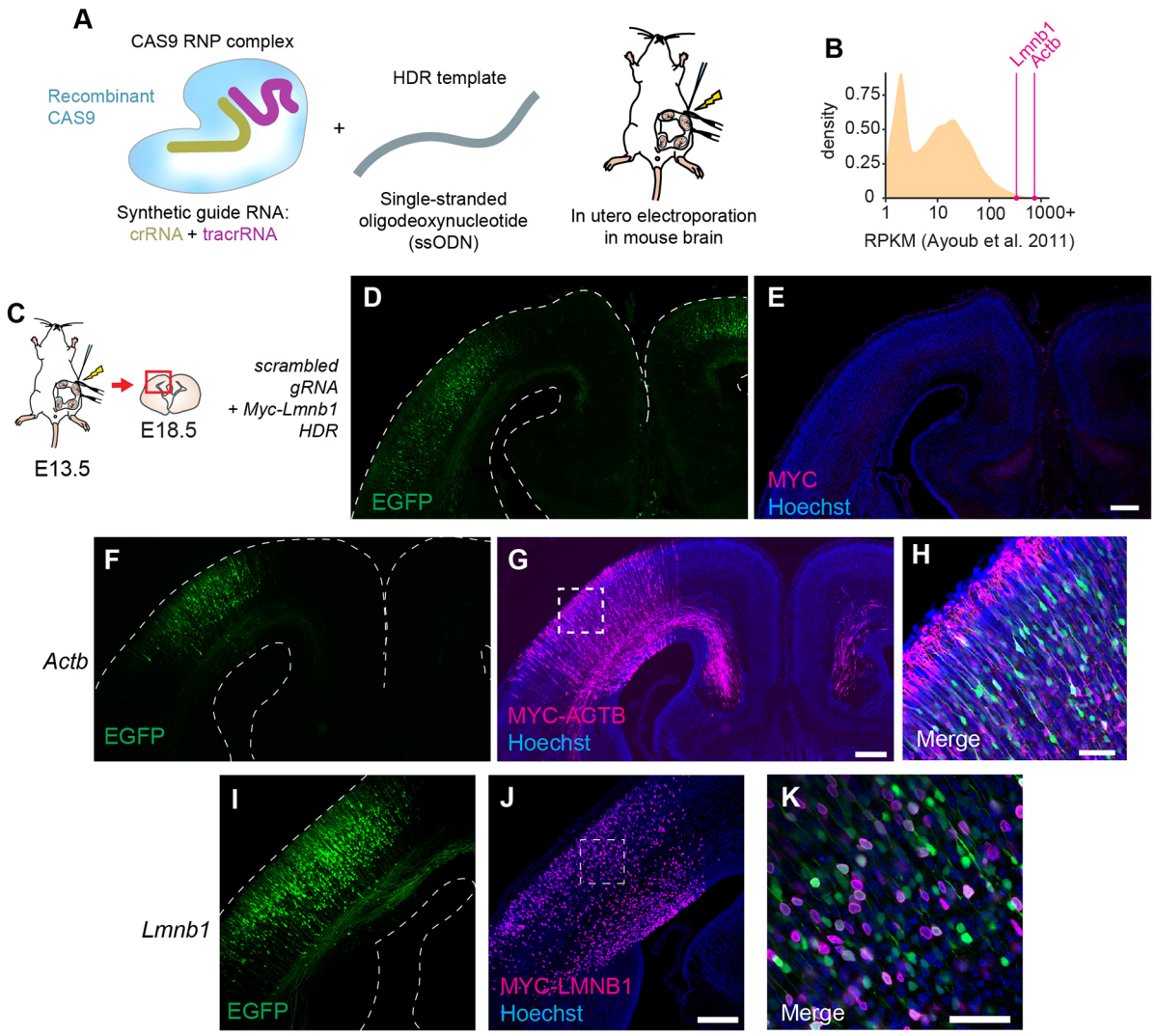

Fig. 1. Examples of Breasi-CRISPR results 5 days after electroporation. (A) Diagram representing Breasi-CRISPR constituents. (B) Graph showing relative reads per kilobase of exon model per million mapped reads (RPKM) for *Lmnb1* and *Actb* (data from Ayoub et al., 2011). (C) Diagram outlining the approach for the experiments shown in D-I. Breasi-CRISPR IUE was performed at E13.5 followed by sample collection at E18.5 and histological analysis of coronal sections. (D,E) Representative confocal images of Breasi-CRISPR control using a scrambled gRNA with Myc-Lmnb1 repair template showing a lack of MYC signal (fuchsia) without directed endonuclease activity. (F-H) Representative confocal images of Breasi-CRISPR-tagged MYC-ACTB (fuchsia) in electroporated neurons (green). (I-K) Representative confocal images of Breasi-CRISPR-tagged MYC-LMNB1 (fuchsia) in electroporated neurons (green). Dashed lines delineate brain outer surface and ventricles. Images are representative of at least three brains across several litters. Scale bars: 200 µm (D-G,I,J); 50 µm (H,K).

the detection of protein–protein interactions consistent with the previously known role of the tagged protein. Thus, this technique can be used to interrogate the function of endogenous proteins during early brain development.

RESULTS

Breasi-CRISPR is an efficient method to epitope-tag various endogenous proteins in the embryonic mouse cortex

As a first test of the efficacy of this technique, we used Breasi-CRISPR to epitope-tag the abundant, ubiquitous proteins β-actin and lamin B1 (encoded by the *Actb* and *Lmnb1* genes, respectively). Of note, we used published RNA-sequencing (RNA-seq) data from microdissected E14.5 mouse cortices as a proxy for overall protein abundance at the targeted time point (Fig. 1B) (Ayoub et al., 2011). β-Actin is a cytoskeletal protein important throughout cortical development both in progenitors and neurons (Lian and Sheen, 2015). Lamin B1 is a nuclear lamina protein responsible for maintaining nuclear architecture, DNA replication and gene expression (David, 2011). We used single-stranded oligodeoxynucleotide (ssODN) HDR templates to integrate the MYC-tag sequence immediately downstream of the translation start site of the *Actb* and *Lmnb1* genes. IUE was performed at E13.5, together with a plasmid expressing EGFP to visualize transfected cells (Fig. 1C). Our initial analysis of Breasi-CRISPR-targeted cortices was performed at E18.5, 5 days after the electroporation, because we hypothesized that it would take time for CRISPR reagents to introduce the MYC sequence into the targeted loci, and for cells to express the tagged endogenous proteins. For both gene targets, IHC targeting the MYC-tag consistently showed a very large number of cells with positive signal. As expected, MYC-ACTB signal showed filamentous structures present in the cytoplasm, and was excluded from nuclei but prominent in axons crossing the midline (Fig. 1F-H). MYC-LMNB1 was observed along the edge of nuclei, consistent with its role as a component of

Development (2022) 149, dev200616. doi:10.1242/dev.200616

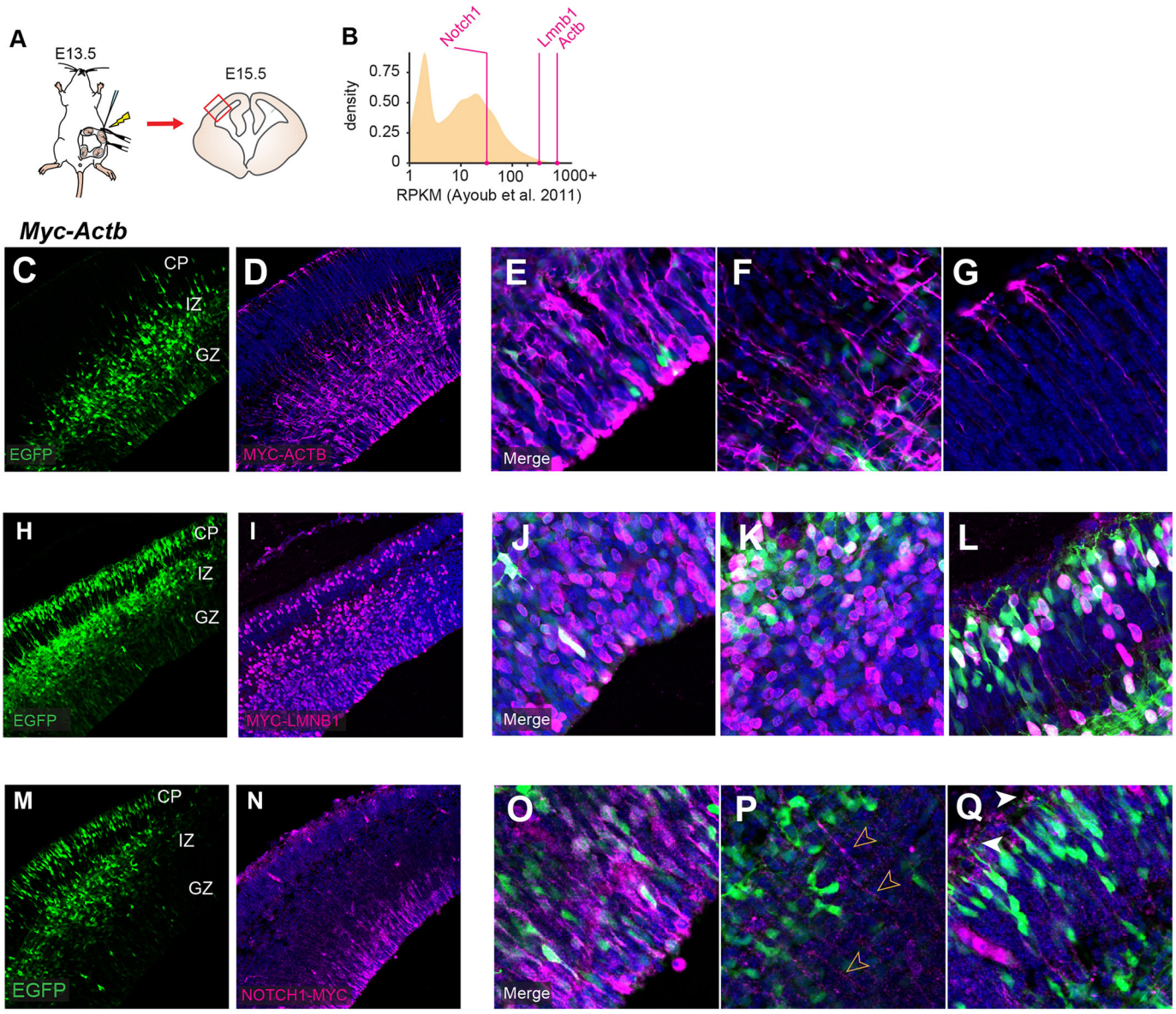

Fig. 2. Examples of Breasi-CRISPR results 2 days after electroporation. (A) Diagram outlining the approach for the experiments shown in C-Q. Breasi-CRISPR IUE was performed at E13.5 followed by sample collection at E15.5 and histological analysis of coronal sections. (B) Graph showing relative reads per kilobase of exon model per million mapped reads (RPKM) for *Notch1*, *Lmnb1* and *Actb* (data from Ayoub et al., 2011). (C-G) Representative confocal images of Breasi-CRISPR-tagged MYC-ACTB (fuchsia) in electroporated neurons (green). Yellow arrowheads (E) point to radial glia actin rings at the ventricular border. (H-L) Representative confocal images of Breasi-CRISPR-tagged MYC-LMNB1 (fuchsia) in electroporated neurons (green). (M-Q) Representative confocal images of Breasi-CRISPR-tagged NOTCH1-MYC (fuchsia) in electroporated neurons (green). Yellow (P) and white (Q) arrowheads point to NOTCH1-MYC signal in radial glia basal processes and endfeet, respectively. Dashed lines delineate inner and outer surface of the cortex. CP, cortical plate; GZ, germinal zone; IZ, intermediate zone. Scale bars: 100 µm (C,D,H,I,M,N); 30 µm (E-G,J-L,O-Q).

the nuclear lamina (Fig. 1G-I). As a control, we performed Breasi-CRISPR experiments combining a scrambled gRNA with *Myc-Lmnb1* HDR templates. These showed complete absence of MYC signal in the electroporated regions (Fig. 1D,E).

These results prompted us to measure Breasi-CRISPR efficiency within a shorter timeframe following IUE. Therefore, we analyzed signal for MYC-ACTB and MYC-LMNB1 by IHC just 2 days after electroporation at E13.5 (Fig. 2A). Under these conditions, strong MYC-ACTB signal was observed in numerous radial glial cells in the ventricular zone (VZ), as well as in migrating neurons in the subventricular zone (SVZ) and in the intermediate zone (IZ; Fig. 2C-G). In the IZ and in the cortical plate, MYC-ACTB also highlighted radial glial basal processes and endfeet with little to no cytoplasmic EGFP signal (Fig. 2D,G). The lack of EGFP in those structures is a result of low diffusion in thin processes, and demonstrates that tagging endogenous proteins populating distal subcellular compartments may be advantageous to visualize cellular morphology when diffusion of fluorescent proteins is limited.

Although these data demonstrate efficacy of Breasi-CRISPR for highly expressed proteins, such as lamin B1 and β-actin, it was unclear how well it would work for proteins expressed at lower levels. To demonstrate that Breasi-CRISPR works not only with highly expressed proteins, we targeted four genes with lower reported expression levels (Figs 2B,M-Q, 3). We chose *Notch1*, *Fmrp* (*Fmr1*), *Emd* and *Rpl22*, encoding a transmembrane receptor, an RNA-binding protein, another nuclear lamina protein and a

Development (2022) 149, dev200616. doi:10.1242/dev.200616

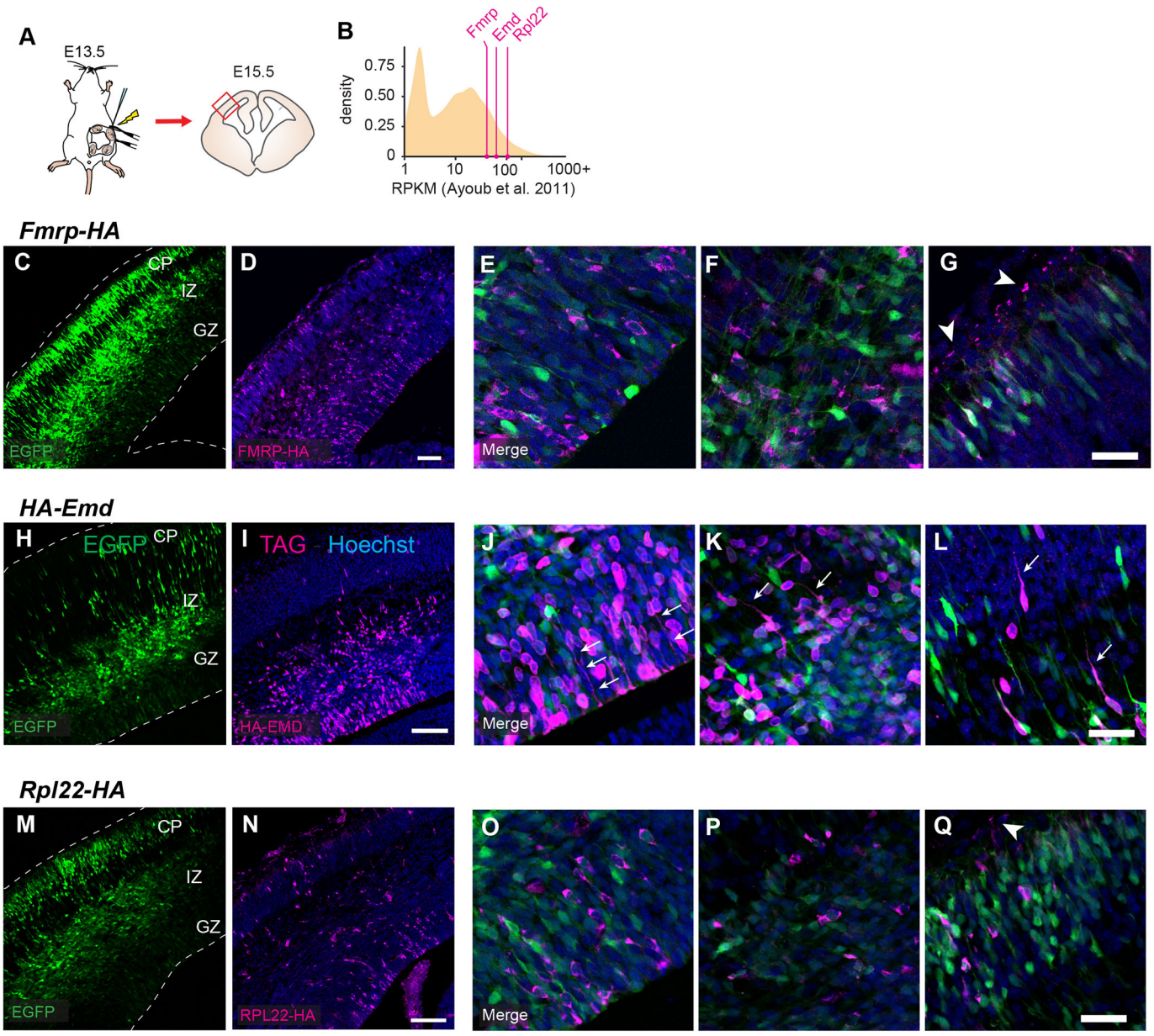

Fig. 3. Further examples of Breasi-CRISPR results 2 days after electroporation. (A) Diagram outlining the approach for the experiments shown in C-Q. Breasi-CRISPR IUE was performed at E13.5 followed by sample collection at E15.5 and histological analysis of coronal sections. (B) Graph showing relative reads per kilobase of exon model per million mapped reads (RPKM) for *Fmrp*, *Emd* and *Rpl22* (data from Ayoub et al., 2011). (C-G) Representative confocal images of Breasi-CRISPR-tagged FMRP-HA (fuchsia) in electroporated neurons (green). White arrowheads (G) point to FMRP-HA signal in radial glia basal endfeet. (H-L) Representative confocal images of Breasi-CRISPR-tagged HA-EMD (fuchsia) in electroporated neurons (green). White arrows (J-L) point to unexpected HA-EMD cytoplasmic signal. (M-Q) Representative confocal images of Breasi-CRISPR-tagged RPL22-HA (fuchsia) in electroporated neurons (green). White arrowhead (Q) points to RPL22-HA signal in radial glia basal endfeet. Dashed lines delineate inner and outer surface of the cortex. CP, cortical plate; GZ, germinal zone; IZ, intermediate zone. Scale bars: 100 µm (C,D,H,I,M,N); 30 µm (E-G,J-L,O-Q).

ribosomal protein, respectively. In most cases, we selected where to insert tags within proteins based on previously published data for the protein of interest.

Full-length NOTCH1 is a transmembrane receptor protein involved in the regulation of neural progenitor proliferation (Yoon and Gaiano, 2005). Upon binding to its ligand, the C terminus of NOTCH1 is cleaved and transported to the nucleus where it regulates transcription of its target genes. In an attempt to capture both the full length (membrane-bound) and cleaved version (cytoplasmic and nuclear) of NOTCH1 in neural progenitors, we inserted the MYC sequence in the portion of the *Notch1* gene encoding the C terminus of the protein. Two days after IUE, we observed NOTCH1-MYC signal specifically in neural progenitors, with most of the signal showing membrane localization (Fig. 2M-Q). Although we expected to observe more NOTCH1-MYC signal in progenitor nuclei, this could be explained by the known short half-life of the intracellular domain compared with that of the full-length protein at the membrane (Carrieri and Dale, 2016). Of note, we observed NOTCH1-MYC signal not only in radial glia soma and apical endfeet, but also in their basal processes and endfeet (Fig. 2N,P,Q). This suggests that NOTCH1 may have an underexplored role in those structures.

Development (2022) 149, dev200616. doi:10.1242/dev.200616

Next, we inserted an HA-tag sequence immediately upstream of the stop codon of *Fmrp*. FMRP is an RNA-binding protein that controls diverse aspects of mRNA metabolism such as translation and localization. It has been reported to be ubiquitously expressed in the developing cortex with a specific enrichment in radial glia apical and basal endfeet (Saffary and Xie, 2011; Pilaz et al., 2016a). As expected, FMRP-HA was mainly observed in the cytoplasm of targeted cells (Fig. 3C-G). In radial glia, strong signal was observed in apical endfeet as well as in basal endfeet (Fig. 3D,G), as observed previously (Saffary and Xie, 2011; Pilaz et al., 2016a).

Emd encodes emerin, a nuclear membrane protein and a component of the nuclear lamina (Koch and Holaska, 2014). We used Breasi-CRISPR to insert an HA-tag sequence in the N terminus of emerin. Two days after electroporation, we observed many cells displaying IHC signal for HA (Fig. 3H-L), resembling the signal we observed for MYC-LMNB1 (Fig. 2H-L). This suggested that the HA-tag sequence was correctly inserted in the *Emd* locus. However, we also observed many cells with localized cytosolic IHC signal. Some radial glia and migrating neurons showed localization in their apical and leading process, respectively (Fig. 3I-L). This could reflect emerin localization outside of the nucleus at adherens junctions, such as in cardiomyocytes (Wheeler et al., 2010), and at the endoplasmic reticulum (Berk et al., 2013; Ostlund et al., 1999), which is consistent with previous data showing endoplasmic reticulum localization in radial glia apical processes and the leading process of migrating neurons (Taverna et al., 2016).

We also successfully added an HA-tag to the C terminus of RPL22 by Breasi-CRISPR. We used this strategy with this specific protein because its endogenous C-terminal tagging has been used to generate the Ribo-tag mouse line (Sanz et al., 2009), enabling the pull down of ribosome-bound RNAs in specific cell types. After 2 days, RPL22-HA signal was cytoplasmic and observed in radial glia as well as migrating neurons (Fig. 3M-Q). Of note, we also observed RPL22-HA signal in the radial glia basal endfeet region within the marginal zone (MZ; Fig. 3Q). The localization of the RPL22-HA signal is in line with the known role of RPL22 and ribosomes in the developing mouse cortex.

Finally, we tested whether CRISPR-tagging could be detected as soon as 24 h after IUE (Fig. 4A). This was performed by Breasi-CRISPR tagging of ACTB or LMNB1, introducing the MYC sequence immediately after the start codons of *Actb* and *Lmnb1*, respectively. We were surprised to observe a significant number of cells displaying MYC signal for both proteins (Fig. 4B-E), suggesting that the genomic integration of the targeted sequence can happen very rapidly after IUE. Altogether, these experiments

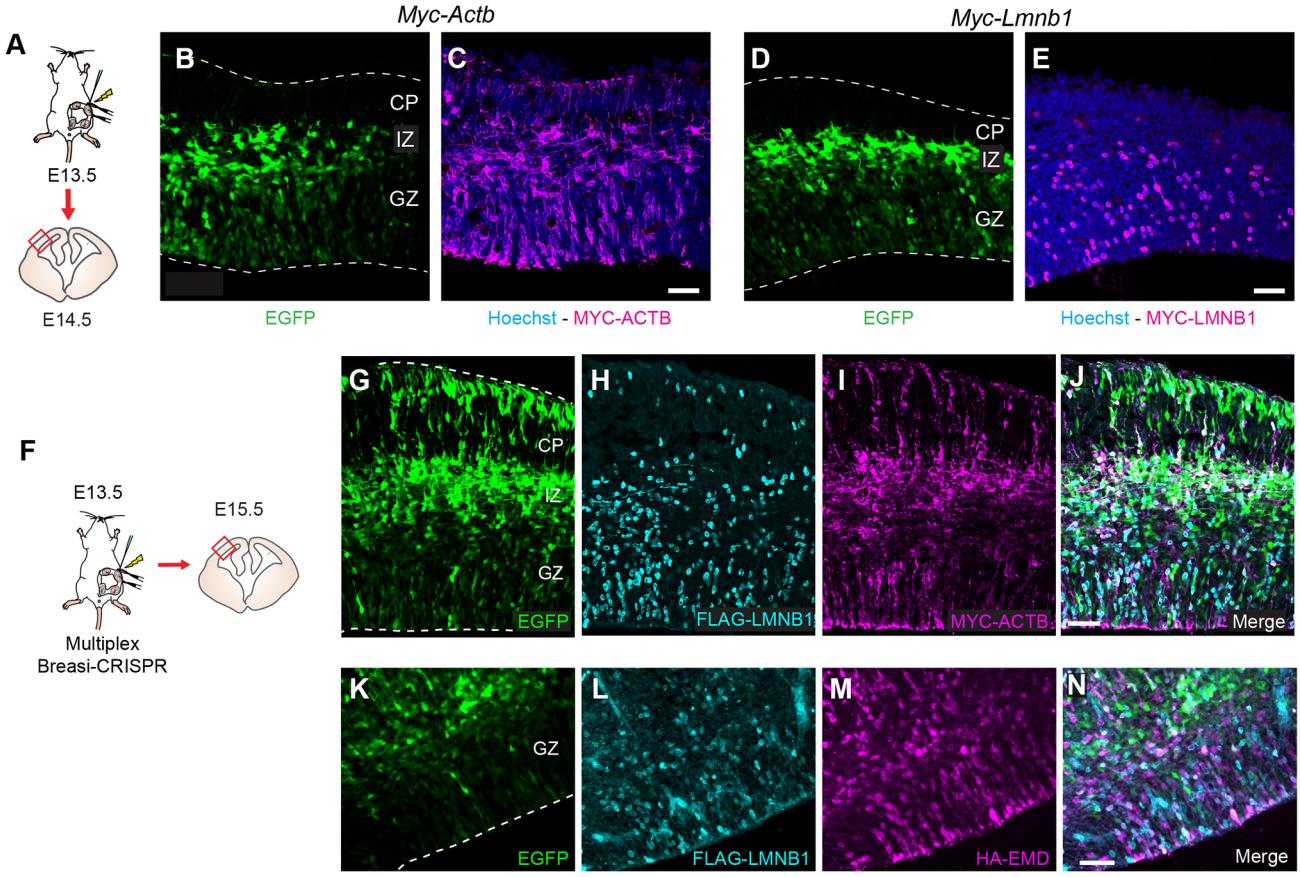

Fig. 4. Examples of Breasi-CRISPR results 1 day after electroporation and multiplexing. (A) Diagram outlining the approach for the experiments shown in B-E. Breasi-CRISPR IUE was performed at E13.5 followed by sample collection at E14.5 and histological analysis of coronal sections. (B,C) Representative confocal images of Breasi-CRISPR-tagged MYC-ACTB (fuchsia) in electroporated neurons (green). (D,E) Representative confocal images of Breasi-CRISPR-tagged MYC-LMNB1 (fuchsia) in electroporated neurons (green). (F) Diagram outlining the approach for the experiments shown in G-N. Breasi-CRISPR IUE was performed at E13.5 followed by sample collection at E15.5 and histological analysis of coronal sections. (G-J) Representative confocal images of multiplex Breasi-CRISPR-tagged FLAG-LMNB1 (turquoise) and MYC-ACTB (fuchsia) in electroporated neurons (green). (K-N) Representative confocal images of multiplex Breasi-CRISPR-tagged FLAG-LMNB1 (turquoise) and HA- EMD (fuchsia) in electroporated neurons (green). Dashed lines delineate inner and outer surface of the cortex. CP, cortical plate; GZ, germinal zone; IZ, intermediate zone. Scale bars: 50 µm.

Development (2022) 149, dev200616. doi:10.1242/dev.200616

highlight that Breasi-CRISPR can be used to tag a variety of endogenous proteins expressed during embryonic development. This will be particularly useful when proteins of interest lack efficient targeting antibodies. This also permits the visualization of those proteins in isolated cells and, thus, provides a more reliable assessment of protein localization within those cells, which can be difficult when proteins of all the cells within a tissue are revealed by IHC.

Multiplexing Breasi-CRISPR

We multiplexed the Breasi-CRISPR approach in order to tag multiple different proteins in the same brain region at the same time. First, we targeted *Lmnb1* and *Actb* simultaneously, adding FLAG- and MYC-tags to LMNB1 and ACTB, respectively (Fig. 4F-J). Next, we targeted LMNB1 and emerin, both proteins of the inner nuclear membrane (Fig. 4K-N). For each, we used two crispr RNAs (crRNAs): one crRNA targeting the *Lmnb1* gene and the other crRNA targeting the *Emd* or the *Actb* genes. Together with these crRNAs, we electroporated two ssODNs: one to add a FLAG-tag in the *Lmnb1* gene and one to add a MYC- or HA-tag in the *Actb* or *Emd* gene, respectively. We performed IUE at E13.5 and collected the samples at E15.5. IHC analyses showed abundant tagging of both proteins, mostly in the same cells (Fig. 4G-N). This demonstrates that Breasi-CRISPR can be used to study the colocalization of multiple proteins within individual cells *in vivo*.

Quantification of Breasi-CRISPR efficiency

To quantify Breasi-CRISPR efficiency, we first used MYC-tagging of lamin B1 because this protein is ubiquitously expressed and its localization in the nucleus facilitates cell counting. We performed

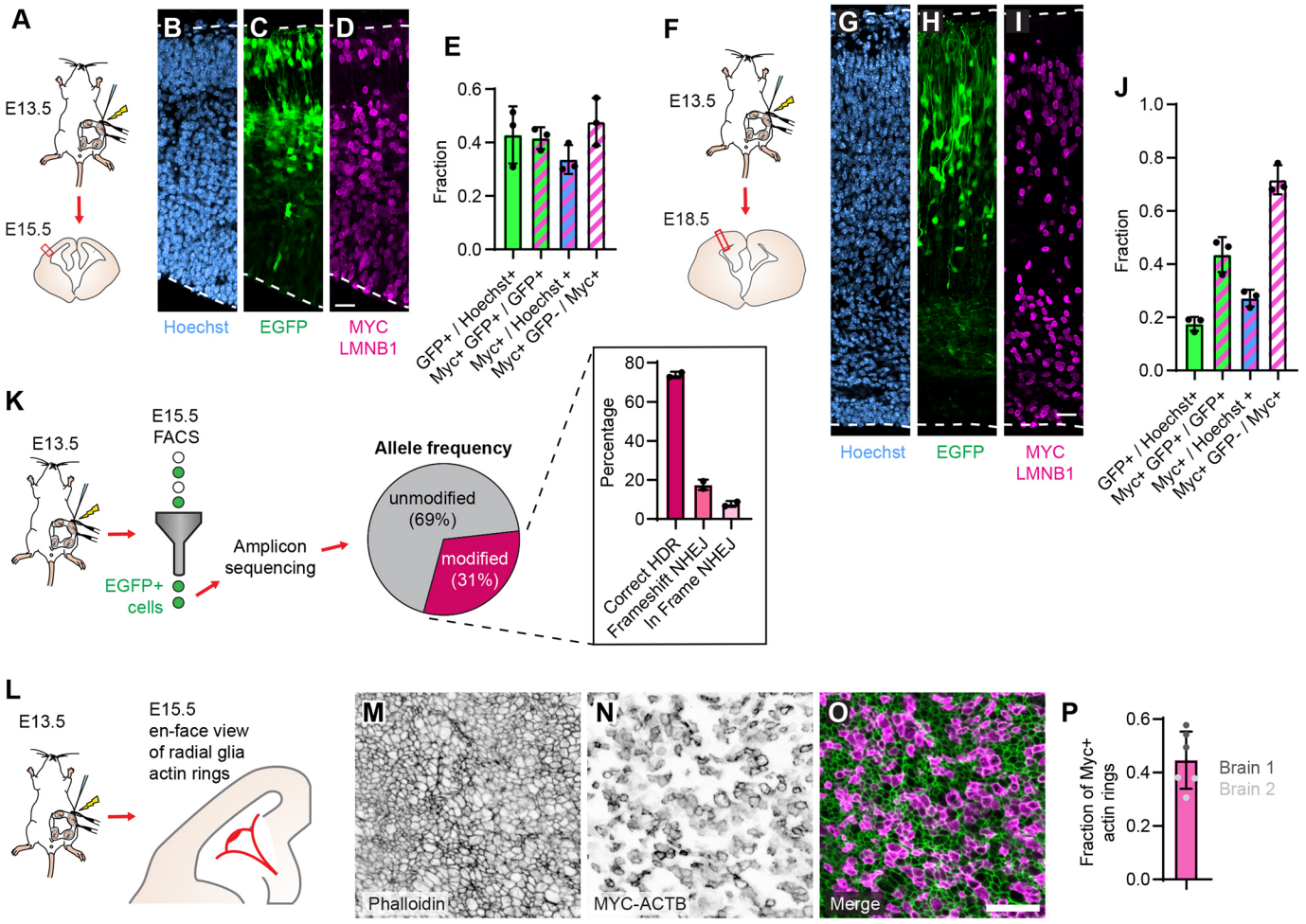

Fig. 5. Quantification of Breasi-CRIPSR efficiency. (A) Diagram outlining the approach for the experiments shown in B-E. Breasi-CRISPR IUE was performed at E13.5 followed by sample collection at E15.5 and histological analysis of coronal sections. (B-D) Representative confocal images of Breasi-CRISPR-tagged MYC-LMNB1 (fuchsia) in electroporated neurons (green) with Hoescht (blue). (E) Quantification of Breasi-CRISPR efficiency by cell counting 2 days after Breasi-CRISPR IUE (n=3 brains from two different litters). (F) Diagram outlining the approach for the experiments shown in G-J. Breasi-CRISPR IUE was performed at E13.5 followed by sample collection at E18.5 and histological analysis of coronal sections. (G-I) Representative confocal images of Breasi-CRISPR-tagged MYC-LMNB1 (fuchsia) in electroporated neurons (green) with Hoechst (blue). (J) Quantification of Breasi-CRISPR efficiency by cell counting 5 days after Breasi-CRISPR IUE (n=3 brains from two different litters). (K) Diagram outlining the approach for sequencing validation. Breasi-CRISPR IUE was performed at E13.5 followed by sample collection at E15.5 with FACS sorting for GFP^+ cells and amplicon sequencing. The percentages of cells with correct HDR, frameshift NHEJ, or in-frame NHEJ were quantified (n=2 litters). (L) Diagram outlining the approach for the experiments shown in M-Q. Breasi-CRISPR IUE was performed at E13.5 followed by sample collection and phalloidin staining of whole-mount cortices. (M-P) Representative confocal images of Breasi-CRIPSR-tagged MYC-ACTB (fuchsia) stained with phalloidin (F-actin stain, green). (P) Quantification of Breasi-CRISPR efficiency by quantification of MYC^+ actin rings (n=2 brains). Data represents mean and s.d. Dashed lines delineate inner and outer surface of the cortex. Scale bars: 25 µm (B-D,G-I); 20 µm (M-O).

Development (2022) 149, dev200616. doi:10.1242/dev.200616

quantifications 2 days and 5 days after IUE at E13.5 (Fig. 5A-J). Within the electroporated region, we counted 43% EGFP$^+$ cells amongst Hoechst$^+$ nuclei, and within these EGFP$^+$ cells, 42% exhibited MYC signal. However, 48% of the MYC$^+$ nuclei were not EGFP$^+$ (Fig. 2B-E). After 5 days, we observed that 17% of Hoechst$^+$ nuclei were EGFP$^+$, and less than half of those EGFP$^+$ nuclei were MYC$^+$; 72% of the MYC$^+$ nuclei were not EGFP$^+$ (Fig. 5F-J). The large fraction of MYC$^+$, EGFP− cells was expected because, although the genomic integration of the MYC sequence is permanent and inherited by all the progeny of targeted progenitors, the cycling progeny of transfected cells lose EGFP expression as a result of the dilution of the plasmid as they progress through multiple cell cycles. This is further supported by the fact that the fraction of MYC$^+$, EGFP$^-$ cells showed a gradual increase over time (Fig. S1A). However, it is possible that increasing the amount of the co-transfected EGFP-expressing plasmid would increase that proportion. Based on Hoechst counterstaining, we also quantified the total fraction of nuclei with efficient Breasi-CRISPR-mediated tagging. We observed that 34% and 27% of all the nuclei were positive for MYC signal after 2 days and 5 days, respectively (Fig. 5E,J). Altogether, these data show that Breasi-CRISPR tagging of proteins in the developing cortex is extremely efficient.

To examine further the efficacy of Breasi-CRISPR, we used amplicon sequencing to quantify the gene-editing products generated by the approach using MYC-LMNB1. We performed IUE at E13.5 and employed fluorescence-activated cell sorting (FACS) at E15.5 to isolate GFP$^+$ cells. Using DNA extracted from these cells, we amplified the region surrounding the Breasi-CRISPR-induced modification by PCR. PCR products were purified and subsequently analyzed by next-generation sequencing (Fig. 5K). The sequencing results showed that out of all the measured *Lmnb1* sequences, 23.4% presented the correct HDR-mediated addition of the MYC-tag sequence to the *Lmnb1* gene. Out of all the modified sequences, which together represented 31% of all the measured sequences, the percentage of correct HDR-modified sequences was greater than 70% (73.8%) and the NHEJ events frequencies were lower than 30% (26.2%), with a fraction of indels leading to frameshifts equal to 17.7% (Fig. 5K). Thus, overall the fraction of amplicons showing NHEJ reached 5.4% amongst all the measured sequences. The occurrence of those frameshifts was also observed indirectly through the measurement of endogenous LMNB1 immunofluorescence signal within EGFP$^+$ cells 5 days after IUE at E13.5. Compared with controls, *Myc-Lmnb1* Breasi-CRISPR-treated cells showed a 7.7% decrease in LMNB1 immunofluorescence signal intensity (Fig. S1B-N), which is consistent with the amplicon sequencing results. Additionally, we observed no overt displacement of endogenous protein localization in targeted brains (Fig. S1B-G,O-W). We used immunofluorescence against the apoptotic marker cleaved caspase 3 (Fig. S2A-M), and analysis of EGFP$^+$ cell positioning comparing control conditions with *Myc-Lmnb1* Breasi-CRISPR treatment 5 days after IUE (Fig. S2N-Q). These two analyses showed no differences between control and Breasi-CRISPR-treated brains. Altogether, these results show that Breasi-CRISPR can efficiently add an epitope-tag to coding sequences in the embryonic cortex within 1 day of IUE with minimal generation of indels that could be deleterious for the expression of the gene of interest, and hence the viability of the targeted cells. This makes it ideal for studying proteins that are expressed transiently during development.

As another means to test Breasi-CRISPR efficacy using another gene target, we analyzed MYC-ACTB signal together with the F-actin marker phalloidin in wholemounts of electroporated cortices, focusing on the ventricular border 2 days after IUE (Fig. 5L-P). This allowed us to visualize MYC-ACTB$^+$, Phalloidin$^+$ 'actin-rings' localized at radial glia apical endfeet. Measuring the fraction of MYC-ACTB$^+$, Phalloidin$^+$ endfeet within the whole Phalloidin$^+$ population, this approach enabled us to quantify the fraction of radial glia in which β-actin was epitope-tagged by Breasi-CRISPR. In the electroporated regions, we counted that 30% to 57% of all Phalloidin-labeled apical endfeet showed MYC-ACTB signal. Altogether, these data demonstrate the rapid efficacy of the Breasi-CRISPR approach.

Live imaging of endogenous proteins fused to fluorescent proteins via Breasi-CRISPR

Next, we performed a set of experiments to show that Breasi-CRISPR allows the knock-in of larger tags such as EGFP, thus enabling live-imaging studies of endogenous proteins during cortical development. For this, we used ssODNs with EGFP-tag and sequence targeting the *Lmnb1* gene. These ssODNs were generated in-house using the ivTRT ('*in vitro* transcription and reverse transcription') method (Quadros et al., 2017; Miura et al., 2018). First, IUE was performed at E13.5 and brains were collected and fixed at E18.5, using tdTomato or mCherry expression plasmids as a marker of transfection (Fig. 6A-C). We found that 20% of the tdTomato cells exhibited EGFP-tagged lamin B1 and represented 1% of all the nuclei within the electroporated region. We then visualized Breasi-CRISPR-tagged EGFP-LMNB1 by live imaging in acute embryonic brain slices. Live slices were generated at E15.5, 2 days after the Breasi-CRISPR IUE (Fig. 6D). Live imaging was performed overnight for 20 h. With this approach, we were able to visualize the interkinetic nuclear migration of neural stem cell nuclei in the VZ (Movie 1, Fig. 6G), and the migration of neurons in the SVZ and IZ (Movie 1, Fig. 6F). In migrating neurons, tensions applied to nuclei as the cells migrate through dense tissue was evident (Fig. 6F). To demonstrate potential applications for Breasi-CRISPR, we quantified the interkinetic nuclear migration of EGFP-LMNB1$^+$ radial glia (Fig. 6H). These results were consistent with those observed by others (Tsai et al., 2010). Altogether, these data demonstrate that Breasi-CRISPR can be utilized to visualize endogenous protein dynamics during embryonic cortical development. This provides a powerful approach that is not reliant on exogenous expression of proteins or transgenic mouse lines.

Using Breasi-CRISPR to study protein–protein interactions

Given the efficiency we observed by IHC, we were encouraged to test whether the Breasi-CRISPR technique would enable us to perform in-depth protein studies using tagged proteins in the developing cortex. First, we attempted to detect tagged proteins using immunoblot analyses of lysates 2 days after IUE at E13.5 (Fig. 7A). For MYC-actin (Fig. 7B), MYC-lamin B1 (Fig. 7D) and HA-EMD (Fig. 7E), we were able to detect the tagged proteins within lysates from one, three and four cortices, respectively. Additionally, we were able to immunoprecipitate MYC-actin using a MYC antibody (Fig. 7C). These data further demonstrate the efficiency of Breasi-CRISPR, prompting us to attempt to use Breasi-CRISPR for downstream high-throughput proteomics studies, such as co-IP. Thus, we performed co-IP mass-spectrometry analyses to reveal interactors of FMRP, a protein of medium abundance (Fig. 3B) in an unbiased fashion. To do this, we used Breasi-CRISPR to knock in the HA-tag immediately upstream of the stop codon of *Fmrp*. We performed IUE at E13.5 and collected cortex samples at E15.5. Pooled cortices from single litters (two litters with five or six embryos per litter) were utilized as technical replicates for co-IP experiments, and co-IPs of non-electroporated cortices were

Development (2022) 149, dev200616. doi:10.1242/dev.200616

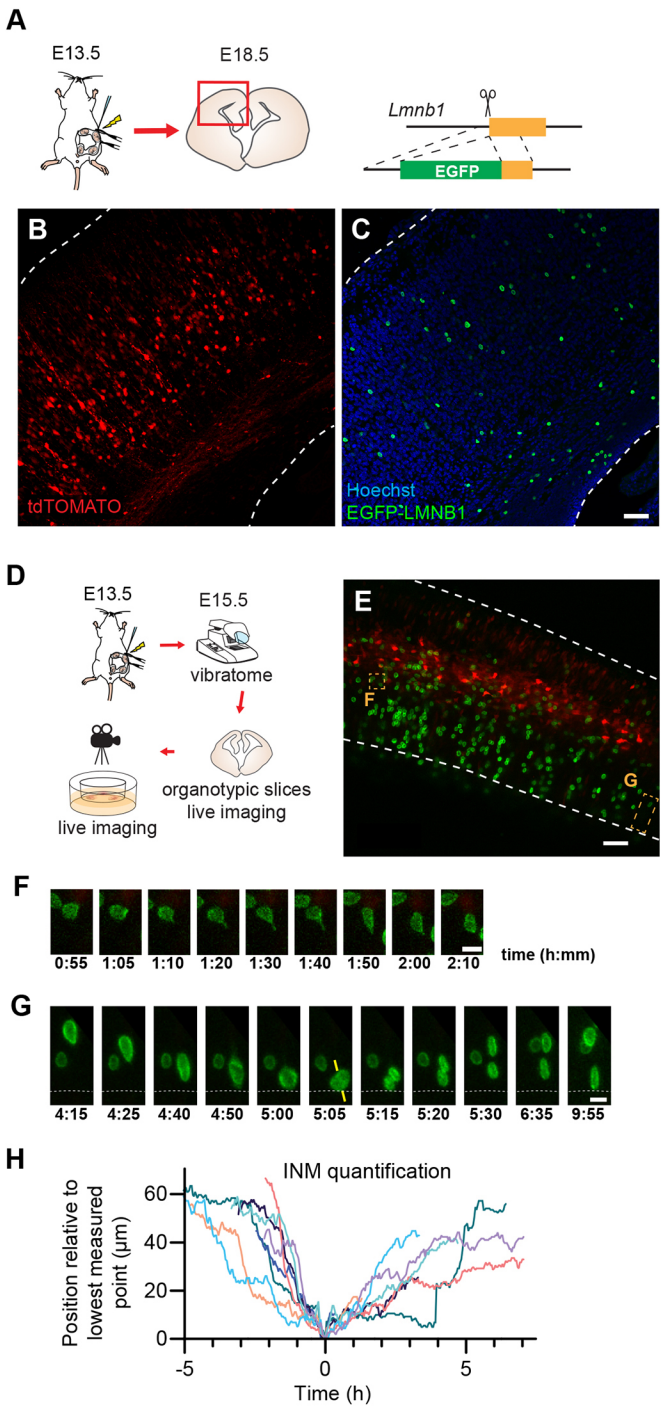

Fig. 6. Fluorescent tagging with Breasi-CRISPR. (A) Diagram outlining the approach for the experiments shown in B,C. Breasi-CRISPR IUE was performed at E13.5 followed by sample collection at E18.5 and histological analysis of coronal sections. (B,C) Representative confocal images of Breasi-CRISPR-tagged EGFP-LMNB1 (green) in electroporated neurons (red). (D) Diagram outlining the approach for the experiments shown in E-G. Breasi-CRISPR IUE was performed at E13.5 followed by sample collection at E15.5, organotypic slice culture and live imaging. (E) Representative confocal image of Breasi-CRISPR-tagged EGFP-LMNB1 (green) in electroporated neurons (red). Dashed lines in B,C,E delineate inner and outer surface of the cortex. (F,G) Representative stills from time-lapse confocal images of Breasi-CRISPR-tagged EGFP-LMNB1 (green), taken from the regions shown by dashed boxes in E. Yellow bars (G) indicate mitotic cleavage plane. (H) Quantification of interkinetic nuclear migration (INM) in the EGFP-LMNB1-positive cells shown in E-G. Each colored line represents the imaged position of EGFP-LMNB1-positive radial glia as they progress through interkinetic nuclear migration. Scale bars: 50 µm (B,C,E); 5 µm (F,G).

used as controls (Fig. 8A,B). Consistent with the known role of FMRP in the regulation of mRNA translation, gene ontology analyses of proteins significantly enriched in the co-IP fractions from FMRP-HA cortices showed an over-representation of networks linked to mRNA processing, especially for ribosomes and the spliceosome (Fig. 8C-E, Table S1). We also observed an enrichment of intermediate filament proteins, which are regulated by FMRP (Thomsen et al., 2013). Surprisingly, we also found a network specific to complement activation. We were also initially surprised to discover an enrichment for a network of histone proteins; however, direct interactions between FMRP and this subclass of protein have been reported (Alpatov et al., 2014). Altogether, this demonstrates that Breasi-CRISPR can be used to reveal protein–protein interactions in the developing mouse cortex.

DISCUSSION

In this study, we describe Breasi-CRISPR, an improved approach combining IUE with CRISPR technology, to tag endogenous proteins in the developing mouse cortex. Breasi-CRISPR enabled us to tag proteins in up to 30% of all the cells within the electroporated area. Tagged proteins can be visualized by IHC as soon as 1 day following electroporation and by immunoblotting as soon as 2 days after IUE. Breasi-CRISPR also shows multiplexing capacity and enables the insertion of fluorescent tags to visualize the dynamics of endogenous protein in large numbers of cells, by imaging in live tissue. Moreover, using tagged FMRP as a bait, we demonstrate that Breasi-CRISPR can be utilized to interrogate protein–protein interactions by co-IP of tagged proteins. Current methods for these approaches rely upon effective antibodies, which may not be available for a protein of interest, or on overexpression of tagged proteins, which can lead to non-specific binding. By overcoming those challenges, this technique will propel an understanding of cortical development by allowing specific detection of endogenous protein expression.

Published approaches coupling CRISPR technology with IUE to tag endogenous proteins rely on plasmids encoding the CAS9 protein and the gRNA (Tsunekawa et al., 2016; Suzuki et al., 2016; Mikuni et al., 2016; Uemura et al., 2016; Fang et al., 2021). Thus, there is a significant lag between electroporation and the production of CAS9 within electroporated cells, emanating from the need for the plasmid to integrate the nucleus, followed by transcription of the mRNA encoding CAS9, the export of this mRNA to the cytoplasm and finally its translation. Given that integration of the plasmid into the nucleus requires the cells to accomplish mitosis soon after IUE (Stancik et al., 2010; Pilaz et al., 2009), using plasmids encoding CRISPR reagents limits the number of cells eventually expressing CAS9 and the gRNA. With the Breasi-CRISPR approach, however, a pre-formed CAS9/gRNA complex is directly delivered into the cells and is capable of targeting the genome immediately. Moreover, as the gRNAs are synthetic, they can be chemically enhanced to promote their stability, thereby maintaining high levels in targeted cells for longer periods of time. This is also true for single-stranded HDR templates. However, owing to cost, longer ssODN HDR templates introducing fluorescent tags are usually generated in-house through ivTRT (Quadros et al., 2017). In this case, to our knowledge adding stabilizing chemical modifications to the ssODN is not possible, although this could be a valuable avenue of research in the future.

Like any other CRISPR-based approaches, Breasi-CRISPR may have off-target effects in electroporated cells. This can include undesirable editing of other genomic loci owing to sequence homology with the targeted sequence. Because of the error-prone nature of the DNA-repair pathways, this could lead to frameshifts when coding regions are affected, or alteration of critical regulatory regions

Development (2022) 149, dev200616. doi:10.1242/dev.200616

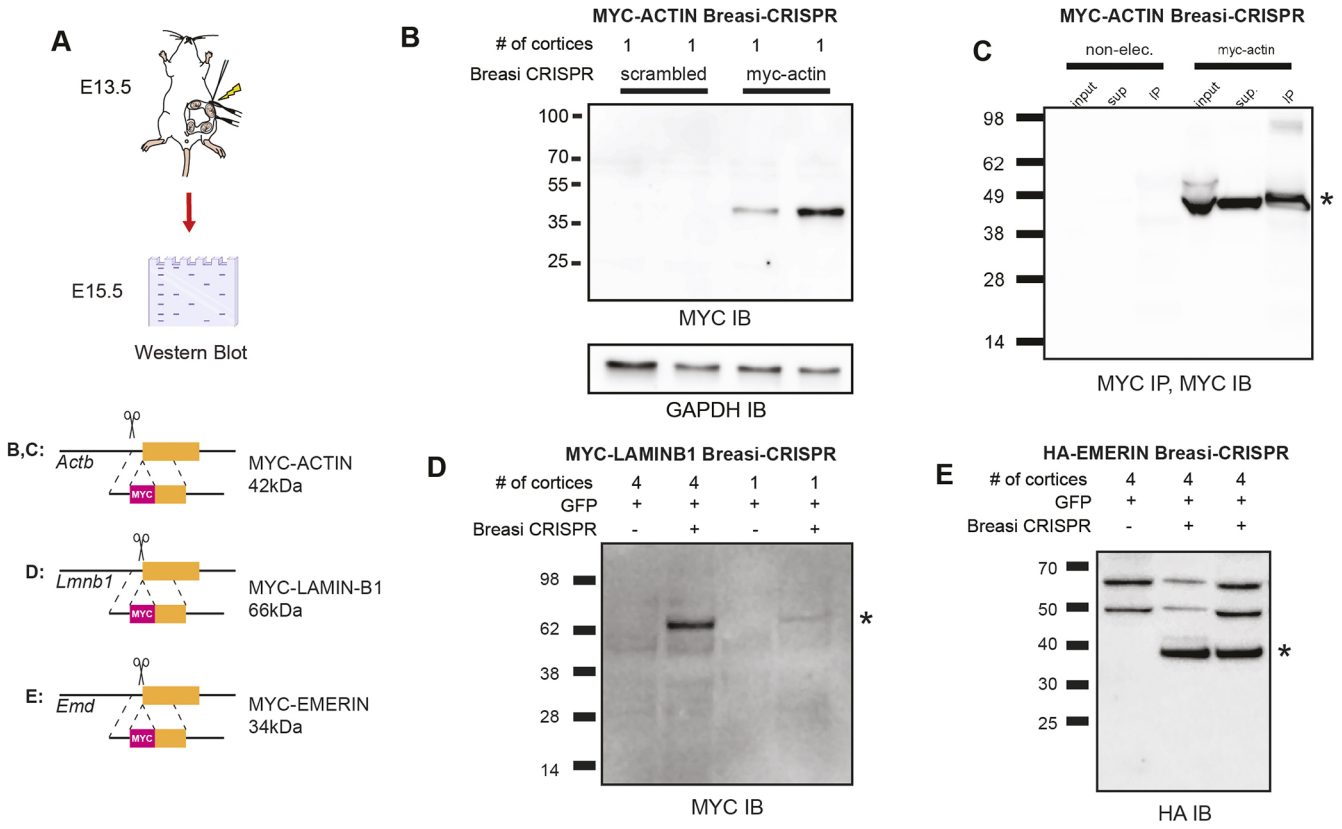

Fig. 7. Visualization of Breasi-CRISPR-tagged proteins by immunoblotting. (A) Diagram outlining the approach for the experiments shown in B-E. Breasi-CRISPR IUE was performed at E13.5 and cortices were collected for immunoblots (IB) at E15.5. Also depicted are schematics indicating the tag insertion with the molecular weight (in kDa) of the protein and tag together. (B) Representative IB showing increased MYC signal in MYC-actin Breasi-CRISPR-electroporated samples compared with samples electroporated with scrambled gRNA and Myc-Actin repair template. Lower panel shows IB targeting GAPDH as a loading control. (C) Representative IB showing enrichment of MYC signal in MYC-actin Breasi-CRISPR-electroporated samples compared with samples electroporated with GFP alone. (D) Representative IB showing increased MYC signal in MYC-lamin B1 Breasi-CRISPR-electroporated samples compared with samples electroporated with GFP alone, and an increase when four cortices are pooled compared with one cortex alone. (E) Representative IB showing increased HA signal in HA-EMERIN Breasi-CRISPR-electroporated samples compared with samples electroporated with GFP alone. IP, immunoprecipitation. Asterisks mark bands at the approximate expected molecular weight for the respective tagged protein.

when non-coding regions are disrupted. Many online algorithms allow the experimenter to predict gRNA off-target sequences, enabling mitigation at the design level. However, undesirable editing could also occur in the targeted region itself owing to potential inefficiency of the HDR-based approach. We tested this directly (1) through sequencing of the targeted region and observed NHEJ-induced frameshifts in 5% of all the sequenced fragments (compared with 23% for correct HDR) and (2) through the measurement of endogenous protein levels in electroporated cells (Fig. S1B-W). Altogether, this suggests that, overall, this effect may be minimal. However, it is important to consider scenarios in which one allele has been successfully tagged and the other allele has a frameshift mutation. In this case, the frameshift mutation could affect the localization of the tagged protein. Finally, we did not see any increase of apoptosis in electroporated brains (Fig. S2A-M), and the distribution of $EGFP^{+}$ cells did not seem to be altered (Fig. S2N-Q). This suggests that Breasi-CRISPR does not have overt noxious effects.

Most of our Breasi-CRISPR designs worked efficiently without the need for optimization. However, some required us to test different conditions to find tags and positions within the proteins to enable their visualization by IHC or immunoblotting. We assumed that this is because certain epitope-tags can lead to instability of the protein (Saiz-Baggetto et al., 2017). Additionally, sequences surrounding the epitope-tag can hinder their accessibility to antibodies (Schüchner et al., 2020). One way to mitigate this issue is to add a linker sequence between the tag and the protein (Chen et al., 2013). Moreover, the target protein may be cleaved, leaving the epitope-tag subject to degradation. Finally, the target protein may be expressed at levels so low that its detection might be problematic. In that case, it is possible to add tandem repeats of the tag instead of single copies. Of note, however, the efficiency of the integration might be affected as it is inversely correlated with the size of the inserted sequence (Ohtsuka et al., 2018).

Breasi-CRISPR is expected to work best at earlier developmental time points when progenitors preferentially use HDR over NHEJ for DNA repair (Mikuni et al., 2016). In this study, we performed all the Breasi-CRISPR experiments at E13.5, which is the earliest time at which our group is reproducibly efficient at IUE (75% average success rate). However, the efficacy of the Breasi-CRISPR approach may be further improved when performed at even earlier time points, but will probably decrease at later time points, as observed for the SLENDR (‘single-cell labeling of endogenous proteins by CRISPR/Cas9-mediated homology-directed repair’; Mikuni et al., 2016) approach. This limits the opportunity to target specifically cells born towards the end of corticogenesis, such as upper layer neurons and astrocytes. Another consideration related to the timing of experiments is the age at which electroporated brains are collected. Although we restricted our collections to embryonic stages, there will be great

Development (2022) 149, dev200616. doi:10.1242/dev.200616

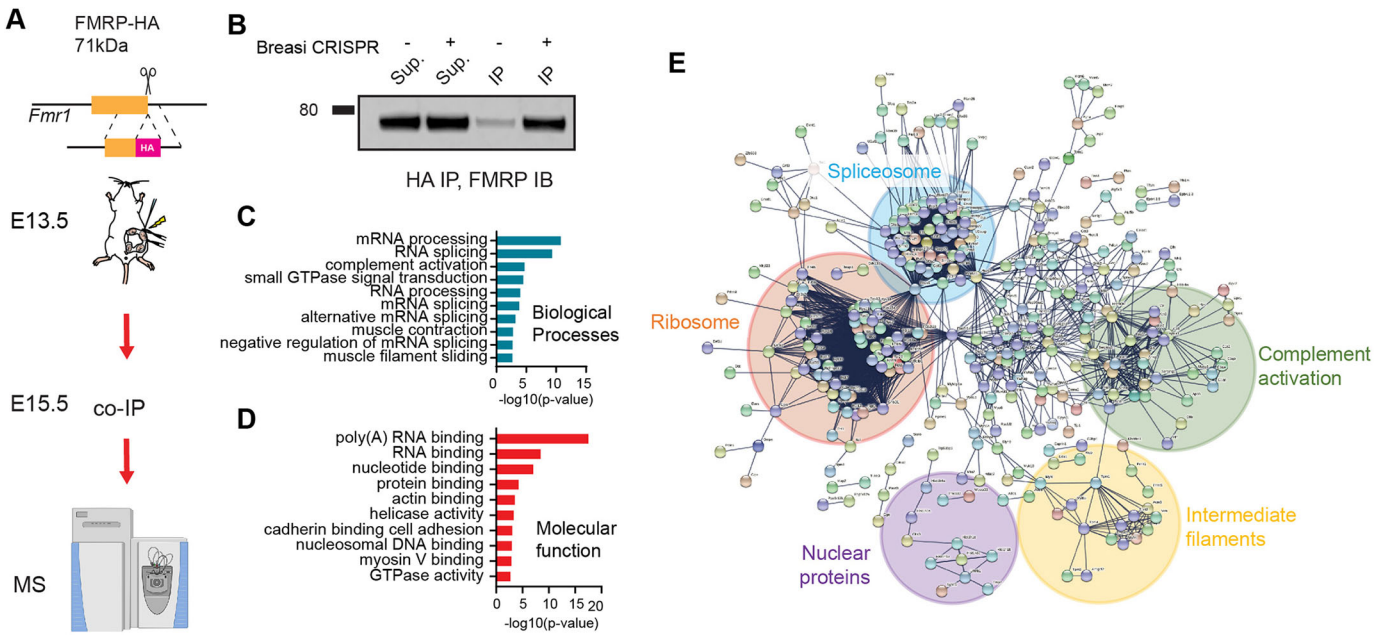

Fig. 8. Example of co-IP/mass spectrometry with Breasi-CRISPR. (A) Diagram outlining the approach for the experiments shown in B-E. FMRP-HA Breasi CRISPR IUE was performed at E13.5 and cortices were collected for co-IP/mass spectrometry (MS) at E15.5. (B) Representative immunoblot (IB) showing enrichment of FMRP signal following HA immunoprecipitation (IP) in FMRP-HA-electroporated samples compared with samples electroporated with GFP alone. (C,D) Gene ontology analyses showing biological processes (C) and molecular functions (D) enriched in FMRP-HA Breasi-CRISPR-electroporated samples. (E) Network analysis of genes enriched in FMRP-HA Breasi-CRISPR from MS analysis.

value in utilizing Breasi-CRISPR to analyze protein localization and interactions in more mature cells during postnatal stages.

In addition to interrogating protein–protein interactions, Breasi-CRISPR should be compatible with RNA-immunoprecipitation to discover the RNA targets of RNA-binding proteins, or with CUT&RUN (‘cleavage under targets & release using nuclease’; Skene and Henikoff, 2017.) to shed light on transcription factor-binding regions in the genome. It may also be possible to couple the protein-tagging capacity of Breasi-CRISPR with other approaches affecting gene expression, such as RNA interference, or overexpression, to test how protein localization and function may be affected by altered expression of other genes. Additionally, multiplexing Breasi-CRISPR for single targets may be possible, enabling the introduction of an epitope-tag and a mutation of interest. For instance, this would enable researchers to assess how mutations of certain genes affect the localization of their encoded proteins. Finally, this approach should be applicable to brain organoids as electroporation-mediated transfection is a viable approach in this system (Lancaster et al., 2013). Leveraging NHEJ and not HDR as presented here, the Clevers lab was able to accomplish this in liver organoids (Artegiani et al., 2020). Therefore, we see no obstacle to transferring Breasi-CRISPR to brain organoids as well. Together, we anticipate that the multiple applications of Breasi-CRISPR will be a powerful approach enabling researchers to interrogate basic mechanisms related to brain development and function.

MATERIALS AND METHODS

Animals

All experiments were performed in accordance with Sanford Research IACUC guidelines. C57BL/6J mice were purchased from The Jackson Laboratory and maintained as a breeding colony. Plug dates were defined as E0.5 on the morning the plug was identified. To collect the embryonic brain samples, pregnant females were euthanized by CO_2 inhalation followed by cervical dislocation. Embryonic brains were rapidly collected and evaluated for fluorophore expression under an epifluorescence dissecting microscope (Nikon SMZ3000 stereomicroscope).

IHC

For IHC studies, the embryonic brains were fixed with freshly prepared 4% paraformaldehyde in PBS overnight, cryo-preserved in 30% sucrose in PBS, and frozen in Optimum Cutting Temperature (OCT) compound. Brains were cryo-sectioned at 20 µm and attached to charged slides. For IHC, sections were permeabilized using 0.5% Triton X-100 in PBS for 20 min and washed in PBS. The sections were blocked in 10% normal goat serum and 1% bovine serum albumin in PBS for 1 h, washed with PBS, and incubated in primary antibody overnight at 4°C. Following PBS washes, sections were incubated with an Alexa Fluor-conjugated secondary antibody and Hoechst 33342 for 1 h at room temperature (RT), washed in PBS, and mounted in aqueous mounting medium. Antibodies used in this study are listed in Table S1. IHC-treated sections were imaged on a Nikon A1plus inverted confocal microscope using 10×, 20×, 40× and 60× objectives.

Amplicon sequencing

For amplicon sequencing studies, GFP-expressing cortical regions were dissected under an epifluorescence dissecting microscope. Cells were dissociated by cold protease digestion. The cells were FACS-sorted to collect only GFP-expressing cells. Next, cells were lysed, and genomic DNA was collected. PCR was used to amplify the targeted region in the *Lmnb1* gene. Next, adaptor sequences specific to our Illumina sequencing approach were added by PCR. The PCR product was purified using AxyPrep Mag PCR Clean-up method. The purity of the eluted DNA was validated using an Agilent 2100 Bioanalyzer, and the samples were sent to the Sanford Burnham Genomics Core Facility for amplicon sequencing.

IP

For IP studies, GFP-expressing cortical regions were dissected under a Nikon SMZ3000 stereomicroscope. The isolated tissue was lysed using NP-40 lysis buffer (50 mM Tris-HCl, pH 7.4 at 4°C, 150 mM NaCl, 1 mM EDTA; supplemented with 0.5% NP-40). Samples were centrifuged at 12,000 rpm (13,800 ***g***) for 15 min, and the supernatant was collected for IP. Magnetic

Development (2022) 149, dev200616. doi:10.1242/dev.200616

beads with Myc or HA antibodies were used to capture Myc- or HA-tagged proteins from the samples by mixing the beads with the samples for 2-3 h at 4°C. The beads bound to the Myc- or HA-tagged proteins were captured using a magnetic stand and washed with TBST (Tris-buffered saline supplemented with 0.1% Tween) before collection into sample buffer for immunoblotting or freezing for mass-spectrometry analysis. Positive hits were identified based on significant enrichment of peptides in the Breasi-CRISPR electroporated samples compared with non-electroporated samples. There were two replicates per condition. Enrichment was deemed significant when peptides were observed only in Breasi-CRISPR electroporated samples or when the *P*-value for a *t*-test comparing the label-free quantitation (LFQ) intensities between electroporated and non-electroporated samples was lower than 0.05, and the ratio between the LFQ intensities between electroporated and non-electroporated samples was greater than 1.

Immunoblot analyses

Samples lysed with NP-40 or RIPA buffer were loaded on 4-12% Bolt bis-tris gels and subjected to electrophoresis for 1 h at 200 V. The proteins were transferred to nitrocellulose membranes using the Power Blotter system, blocked with 5% milk for 1 h, and incubated with primary antibody overnight at 4°C. Blots were washed with TBST, incubated with HRP-conjugated secondary antibody for 1 h at room temperature, washed in TBST, and chemiluminescence was imaged. Antibodies used for the immunoblot analyses are indicated in Table S1.

IUE

IUE was performed as previously described (Pilaz et al., 2016a). Briefly, E13.5 pregnant mice were anesthetized using isoflurane. An incision was made in the medial ventral abdomen of the pregnant mouse to expose the uterine horns. The Breasi-CRISPR solutions were injected into the lateral ventricles of the embryos and electroporated using tweezer electrodes with the following settings: 60 V, 5 square pulses, 60 ms duration, 1 s intervals. Following the IUE, the uterine horns were returned to the abdominal cavity, the incision was sutured, and the mouse was allowed to recover on a heating pad.

Preparation of Breasi-CRISPR reagents

The design of the crRNA and ssODN combinations was performed using the Alt-R HDR Design tool on the IDT website. Preparation of Breasi-CRISPR reagents for IUE followed the protocol established for the iGONAD protocol (Gurumurthy et al., 2019). Briefly, oligonucliotides and CAS9 were ordered from Integrated DNA Technologies (IDT) using the Alt-R design tools and reagents. This includes a transactivating CRISPR RNA (tracrRNA) (IDT, 1072532), scrambled negative control crRNA (IDT, 1079138) and targeted CRISPR RNA (crRNA) (sequences and catalog numbers in Table S1). The tracrRNA and crRNA (400 µM stock concentration for both) were hybridized in a 1:1 molar solution at 98°C for 2 min then held at room temperature for 10 min, resulting in the final gRNA. The final Breasi-CRISPR solution was composed of: 1.5 µl of gRNA solution (200 µM stock concentration), 2 µl HDR template (200 µM stock solution for synthetic ssODN, 1-3.5 µg/µl for template prepared in-house), 1 µl CAS9 nuclease (IDT, 1081058; stock concentration 10 mg/ml), pCAG-GFP/tdTomato/mCherry (0.6 µg/µl final concentration), 1 µl Fast Green, and RNAase- and DNAase-free water to a final volume of 10 µl. This injection solution was incubated at 37°C for 10-30 min prior to the surgery. Of note, inserts used for EGFP-LMNB1 Breasi-CRISPR experiments were generated in-house using the ivTRT approach (Quadros et al., 2017). PCR primers used to generate the template for *in vitro* transcription can be found in Table S1.

Preparation of live brain slice and live imaging

Brain slices for live imaging were prepared as described previously (Pilaz and Silver, 2014; Pilaz et al., 2016b). Briefly, brains were collected 2 days post-IUE in modified HBSS (1× Hank's Balanced Salt Solution, 2.5 mM Hepes, 20 mM D-glucose and 4 mM $NaHCO_3$) and mounted in agarose prior to sectioning at 300 µm using a vibratome. Slices were transferred to a glass-bottom culture dish coated with collagen and incubated in Slice Culture Medium [DMEM/F12 solution, supplemented with N2 solution and B27 solution (without vitamin A), 5% horse serum and 5% fetal bovine serum, 10 ng/ml FGF]. Brain sections were imaged using a Nikon A1plus inverted confocal microscope. For live-imaging experiments, a *z*-stack covering 70 µm was taken every 5 min for 17 h. During this imaging session, brain slices were kept in a live-imaging chamber maintained at 37°C with 5% CO_2 and humidification within the chamber.

Acknowledgements

We thank Kyle Roux and Indra Chandrasekar for help in experimental design and for sharing reagents, and Debra Silver for reading and providing comments on the manuscript.

Competing interests

The authors declare no competing or financial interests.

Author contributions

Conceptualization: B.L.M., L.-J.P.; Methodology: B.L.M., P.K., N.K.T., C.M.E., L.-J.P.; Validation: B.L.M., C.M.K., L.-J.P.; Formal analysis: B.L.M., P.K., N.K.T., C.M.K., L.-J.P.; Investigation: B.L.M., P.K., N.K.T., C.M.K., A.K., L.-J.P.; Resources: C.M.E., L.-J.P.; Data curation: B.L.M., P.K., N.K.T., C.M.K., L.-J.P.; Writing - original draft: B.L.M., N.K.T., L.-J.P.; Writing - review & editing: B.L.M., N.K.T., C.M.K., L.-J.P.; Visualization: B.L.M., P.K., N.K.T., C.M.K., L.-J.P.; Supervision: L.-J.P.; Project administration: L.-J.P.; Funding acquisition: B.L.M., L.-J.P.

Funding

This research was funded by the National Institutes of Health (P20GM103620 to L.J-.P.) and was supported by a fellowship to B.L.M. from the USD Neuroscience, Nanotechnology and Networks program through a grant from the National Science Foundation (DGE-1633213). Deposited in PMC for release after 12 months.

Peer review history

The peer review history is available online at https://journals.biologists.com/dev/lookup/doi/10.1242/dev.200616.reviewer-comments.pdf.

References

Alpatov, R., Lesch, B. J., Nakamoto-Kinoshita, M., Blanco, A., Chen, S., Stützer, A., Armache, K. J., Simon, M. D., Xu, C., Ali, M. et al. (2014). A chromatin-dependent role of the fragile X mental retardation protein FMRP in the DNA damage response. *Cell* **157**, 869-881. doi:10.1016/j.cell.2014.03.040

Artegiani, B., Hendriks, D., Beumer, J., Kok, R., Zheng, X., Joore, I., Chuva De Sousa Lopes, S., Van Zon, J., Tans, S. and Clevers, H. (2020). Fast and efficient generation of knock-in human organoids using homology-independent CRISPR-Cas9 precision genome editing. *Nat. Cell Biol.* **22**, 321-331. doi:10.1038/s41556-020-0472-5

Ayoub, A. E., Oh, S., Xie, Y., Leng, J., Cotney, J., Dominguez, M. H., Noonan, J. P. and Rakic, P. (2011). Transcriptional programs in transient embryonic zones of the cerebral cortex defined by high-resolution mRNA sequencing. *Proc. Natl. Acad. Sci. USA* **108**, 14950-14955. doi:10.1073/pnas.1112213108

Berk, J. M., Tifft, K. E. and Wilson, K. L. (2013). The nuclear envelope LEM-domain protein emerin. *Nucleus* **4**, 298-314. doi:10.4161/nucl.25751

Carrieri, F. A. and Dale, J. K. (2016). Turn it down a notch. *Front. Cell Dev. Biol.* **4**, 151. doi:10.3389/fcell.2016.00151

Chen, X., Zaro, J. L. and Shen, W.-C. (2013). Fusion protein linkers: property, design and functionality. *Adv. Drug Deliv. Rev.* **65**, 1357-1369. doi:10.1016/j.addr.2012.09.039

David, R. (2011). Nucleoskeleton. Uncovering roles for lamin B. *Nat. Rev. Mol. Cell Biol.* **13**, 3. doi:10.1038/nrm3257

Fang, H., Bygrave, A. M., Roth, R. H., Johnson, R. C. and Huganir, R. L. (2021). An optimized CRISPR/Cas9 approach for precise genome editing in neurons. *Elife* **10**, e65202. doi:10.7554/eLife.65202

Gurumurthy, C. B., Sato, M., Nakamura, A., Inui, M., Kawano, N., Islam, M. A., Ogiwara, S., Takabayashi, S., Matsuyama, M., Nakagawa, S. et al. (2019). Creation of CRISPR-based germline-genome-engineered mice without ex vivo handling of zygotes by i-GONAD. *Nat. Protoc.* **14**, 2452-2482. doi:10.1038/s41596-019-0187-x

Kafri, M., Metzl-Raz, E., Jona, G. and Barkai, N. (2016). The cost of protein production. *Cell Rep.* **14**, 22-31. doi:10.1016/j.celrep.2015.12.015

Kintaka, R., Makanae, K. and Moriya, H. (2016). Cellular growth defects triggered by an overload of protein localization processes. *Sci. Rep.* **6**, 31774. doi:10.1038/srep31774

Koch, A. J. and Holaska, J. M. (2014). Emerin in health and disease. *Semin. Cell Dev. Biol.* **29**, 95-106. doi:10.1016/j.semcdb.2013.12.008

Lancaster, M. A., Renner, M., Martin, C. A., Wenzel, D., Bicknell, L. S., Hurles, M. E., Homfray, T., Penninger, J. M., Jackson, A. P. and Knoblich, J. A. (2013). Cerebral organoids model human brain development and microcephaly. *Nature* **501**, 373-379. doi:10.1038/nature12517

Lian, G. and Sheen, V. L. (2015). Cytoskeletal proteins in cortical development and disease: actin associated proteins in periventricular heterotopia. *Front. Cell Neurosci.* **9**, 99. doi:10.3389/fncel.2015.00099
Mikuni, T., Nishiyama, J., Sun, Y., Kamasawa, N. and Yasuda, R. (2016). High-throughput, high-resolution mapping of protein localization in mammalian brain by in vivo genome editing. *Cell* **165**, 1803-1817. doi:10.1016/j.cell.2016.04.044
Miura, H., Quadros, R. M., Gurumurthy, C. B. and Ohtsuka, M. (2018). Easi-CRISPR for creating knock-in and conditional knockout mouse models using long ssDNA donors. *Nat. Protoc.* **13**, 195-215. doi:10.1038/nprot.2017.153
Ohtsuka, M., Sato, M., Miura, H., Takabayashi, S., Matsuyama, M., Koyano, T., Arifin, N., Nakamura, S., Wada, K. and Gurumurthy, C. B. (2018). i-GONAD: a robust method for in situ germline genome engineering using CRISPR nucleases. *Genome Biol.* **19**, 25. doi:10.1186/s13059-018-1400-x
Ostlund, C., Ellenberg, J., Hallberg, E., Lippincott-Schwartz, J. and Worman, H. J. (1999). Intracellular trafficking of emerin, the Emery-Dreifuss muscular dystrophy protein. *J. Cell Sci.* **112**, 1709-1719. doi:10.1242/jcs.112.11.1709
Pilaz, L. J. and Silver, D. L. (2014). Live imaging of mitosis in the developing mouse embryonic cortex. *J. Vis. Exp.* **88**, 51298. doi:10.3791/51298
Pilaz, L. J., Patti, D., Marcy, G., Ollier, E., Pfister, S., Douglas, R. J., Betizeau, M., Gautier, E., Cortay, V., Doerflinger, N. et al. (2009). Forced G1-phase reduction alters mode of division, neuron number, and laminar phenotype in the cerebral cortex. *Proc. Natl. Acad. Sci. USA* **106**, 21924-21929. doi:10.1073/pnas.0909894106
Pilaz, L. J., Lennox, A. L., Rouanet, J. P. and Silver, D. L. (2016a). Dynamic mRNA transport and local translation in radial glial progenitors of the developing brain. *Curr. Biol.* **26**, 3383-3392. doi:10.1016/j.cub.2016.10.040
Pilaz, L. J., McMahon, J. J., Miller, E. E., Lennox, A. L., Suzuki, A., Salmon, E. and Silver, D. L. (2016b). Prolonged mitosis of neural progenitors alters cell fate in the developing brain. *Neuron* **89**, 83-99. doi:10.1016/j.neuron.2015.12.007
Quadros, R. M., Miura, H., Harms, D. W., Akatsuka, H., Sato, T., Aida, T., Redder, R., Richardson, G. P., Inagaki, Y., Sakai, D. et al. (2017). Easi-CRISPR: a robust method for one-step generation of mice carrying conditional and insertion alleles using long ssDNA donors and CRISPR ribonucleoproteins. *Genome Biol.* **18**, 92. doi:10.1186/s13059-017-1220-4
Saffary, R. and Xie, Z. (2011). FMRP regulates the transition from radial glial cells to intermediate progenitor cells during neocortical development. *J. Neurosci.* **31**, 1427-1439. doi:10.1523/JNEUROSCI.4854-10.2011
Saiz-Baggetto, S., Mendez, E., Quilis, I., Igual, J. C. and Bañó, M. C. (2017). Chimeric proteins tagged with specific 3xHA cassettes may present instability and functional problems. *PLoS One* **12**, e0183067. doi:10.1371/journal.pone.0183067
Sanz, E., Yang, L., Su, T., Morris, D. R., McKnight, G. S. and Amieux, P. S. (2009). Cell-type-specific isolation of ribosome-associated mRNA from complex tissues. *Proc. Natl. Acad. Sci. USA* **106**, 13939-13944. doi:10.1073/pnas.0907143106
Schüchner, S., Behm, C., Mudrak, I. and Ogris, E. (2020). The Myc tag monoclonal antibody 9E10 displays highly variable epitope recognition dependent on neighboring sequence context. *Sci. Signal.* **13**, eaax9730. doi:10.1126/scisignal.aax9730
Skene, P. J. and Henikoff, S. (2017). An efficient targeted nuclease strategy for high-resolution mapping of DNA binding sites. *eLife*, **6**, e21856. doi:10.7554/eLife.21856
Stancik, E. K., Navarro-Quiroga, I., Sellke, R. and Haydar, T. F. (2010). Heterogeneity in ventricular zone neural precursors contributes to neuronal fate diversity in the postnatal neocortex. *J. Neurosci.* **30**, 7028-7036. doi:10.1523/JNEUROSCI.6131-09.2010
Suzuki, K., Tsunekawa, Y., Hernandez-Benitez, R., Wu, J., Zhu, J., Kim, E. J., Hatanaka, F., Yamamoto, M., Araoka, T., Li, Z. et al. (2016). In vivo genome editing via CRISPR/Cas9 mediated homology-independent targeted integration. *Nature* **540**, 144-149. doi:10.1038/nature20565
Taverna, E., Mora-Bermudez, F., Strzyz, P. J., Florio, M., Icha, J., Haffner, C., Norden, C., Wilsch-Brauninger, M. and Huttner, W. B. (2016). Non-canonical features of the Golgi apparatus in bipolar epithelial neural stem cells. *Sci. Rep.* **6**, 21206. doi:10.1038/srep21206
Thomsen, R., Pallesen, J., Daugaard, T. F., Børglum, A. D. and Nielsen, A. L. (2013). Genome wide assessment of mRNA in astrocyte protrusions by direct RNA sequencing reveals mRNA localization for the intermediate filament protein nestin. *Glia* **61**, 1922-1937. doi:10.1002/glia.22569
Tsai, J.-W., Lian, W.-N., Kemal, S., Kriegstein, A. R. and Vallee, R. B. (2010). Kinesin 3 and cytoplasmic dynein mediate interkinetic nuclear migration in neural stem cells. *Nat. Neurosci.* **13**, 1463-1471. doi:10.1038/nn.2665
Tsunekawa, Y., Terhune, R. K., Fujita, I., Shitamukai, A., Suetsugu, T. and Matsuzaki, F. (2016). Developing a de novo targeted knock-in method based on in utero electroporation into the mammalian brain. *Development* **143**, 3216-3222. doi:10.1242/dev.136325
Uemura, T., Mori, T., Kurihara, T., Kawase, S., Koike, R., Satoga, M., Cao, X., Li, X., Yanagawa, T., Sakurai, T. et al. (2016). Fluorescent protein tagging of endogenous protein in brain neurons using CRISPR/Cas9-mediated knock-in and in utero electroporation techniques. *Sci. Rep.* **6**, 35861. doi:10.1038/srep35861
Wheeler, M. A., Warley, A., Roberts, R. G., Ehler, E. and Ellis, J. A. (2010). Identification of an emerin-β-catenin complex in the heart important for intercalated disc architecture and β-catenin localisation. *Cell. Mol. Life Sci.* **67**, 781-796. doi:10.1007/s00018-009-0219-8
Yoon, K. and Gaiano, N. (2005). Notch signaling in the mammalian central nervous system: insights from mouse mutants. *Nat. Neurosci.* **8**, 709-715. doi:10.1038/nn1475